AAS 15-359

AN RBF-COLLOCATION ALGORITHM FOR ORBIT PROPAGATION

Tarek A. Elgohary,[*] John L. Junkins[†] and Satya N. Atluri[‡]

Several analytical and numerical methods exist to solve the orbit propagation of the two-body problem. Analytic solutions are mainly implemented for the unperturbed/classical two-body problem. Numerical methods can handle both the unperturbed and the perturbed two-body problem. The literature is rich with numerical methods addressing orbit propagation problems such as, Gauss-Jackson, higher order adaptive Runge-Kutta and Talyor series based methods. More recently, iterative methods have been introduced for orbit propagation based on the Chebyshev-Picard methods. In this work, Radial Basis Functions, RBFs, are used with time collocation to introduce a fast, accurate integrator that can readily handle orbit propagation problems. Optimizing the shape parameter of the RBFs is also introduced for more accurate results. The algorithm is also applied to Lambert's problem. Two types of orbits for the unperturbed two-body problem are presented; (1) a Low Earth Orbit (LEO) and (2) a High Eccentricity Orbit (HEO). The initial conditions for each orbit are numerically integrated for 5, 10 and 20 full orbits and the results are compared against the Lagrange/Gibbs *F&G* analytic solution, *Matlab ode45* and the higher order *rkn12(10)*. A Lambert's orbit transfer numerical example is also introduced and the results are compared against the *F&G* solution. The algorithm is shown to be capable of taking large time steps while maintaining high accuracy which is very significant in long-term orbit propagation problems.

INTRODUCTION

The equation of motion for the relative two-body problem is given by,

$$\ddot{\mathbf{r}} = -\frac{\mu}{r^3}\mathbf{r} + \mathbf{a}_d \tag{1}$$

where, μ is the gravitational parameters, $\mathbf{r} = \begin{bmatrix} x & y & z \end{bmatrix}^{\mathrm{T}}$ is the position vector in the inertial frame, $r = \sqrt{x^2 + y^2 + z^2}$, and $\mathbf{a}_d$ is the perturbation acceleration. Equation (1) can be recast as a general 1st order system of ordinary differential equations as,

$$\dot{\boldsymbol{\chi}} = \mathbf{g}\left(\boldsymbol{\chi}\right) \tag{2}$$

where $\boldsymbol{\chi} \equiv \begin{bmatrix} x & y & z & \dot{x} & \dot{y} & \dot{z} \end{bmatrix}^{\mathrm{T}}$. For the unperturbed/classical two-body problem, $\mathbf{a}_d = \mathbf{0}$, Eq. (1) has an analytic solution extracted from the the conservation of angular momentum and the fundamental orbit integrals.[1,2] Similarly, the Lagrange/Gibbs, *F&G*, solution exploits the conservation of angular momentum to express the future state vector as a linear combination of the initial

[*]Department of Aerospace Engineering, Texas A&M University, College Station, TX. Currently visiting graduate student, University of California Irvine. AAS/AIAA Student Member.

[†]Department of Aerospace Engineering, Texas A&M University, College Station, TX. Founding Director Texas A&M Institute for Advanced Study

[‡]Center for Aerospace Research & Education, University of California, Irvine. Also Fellow & Eminent Scholar, Texas A&M Institute for Advanced Study, Texas A&M University, College Station, TX.

conditions.[1,2] The recursion of the equation produced by successive differentiation has also been explored to produce a power series based solution with Lagrange Fundamental Invariants.[1]

An analytic continuation power series based solution is also introduced by defining two scalar kinematic variables that improved the classical series convergence and enabled multiple orbits propagation while maintaining very high solution accuracy.[3] The stability of the series is then further investigated with Padé series approximation to better understand the convergence properties of the series solution.[4] Furthermore, and based on the series approximation analytic state transition tensor models are derived up to third order to handle the J_2 perturbation.[5] Most recently, the addition of Horner backwards summation scheme as well as variable step size algorithms showed significant improvements to the performance and accuracy of the analytic continuation technique for the higher order perturbations.[6,7]

Several numerical techniques exist to handle the solution of the nonlinear initial value problem (IVP) in Eq. (2). The Runge-Kutta, *RK*, family of methods can be considered as the most widely used explicit methods for numerical integration. The classical or the 4th-order *RK* method is the most commonly used among various *RK* methods. Adaptive step-size 4th-order *RK* methods are developed and are known as the Runge-Kutta-Fehlberg, *RKF*, methods.[8] Higher order adaptive *RK* methods are then developed for high accuracy requirement applications. Adaptive Runge-Kutta-Nyström, *RKN*, methods with order 8(7), 9(8), 10(9) and 11(10) are developed to solve general second-order ordinary differential equations.[9] For orbit propagation problems, the Gauss-Jackson method is studied extensively and compared against other numerical techniques, e.g. *RK4*, *RKN* and Taylor series expansion.[10] It is a predictor-corrector finite difference method designed specifically for solving second order differential equations.[11] The *RKN* 12(10) and 8(6) methods are introduced for general dynamical systems.[12] The method is then compared against several Nyström methods and recursive power series solutions for orbit propagation problems.[13,14] Furthermore, the accuracy of several of the above mentioned numerical integrators are tested in solving different N celestial bodies problems such as, Sun, Jupiter, Saturn, Uranus, and Neptune and nine planets problems.[15] Most of the comparisons performed in the literature addressed the issue of the integration step-size. The need for a high accuracy solution in many cases necessitates a smaller time-step. More recently, Modified Chebyshev-Picard Iteration (MCPI) method has been developed for orbit propagation and general initial value problems.[16,17] The method combines orthogonal basis function, Chebyshev polynomials, with Picard iterations to solve the initial value problem. It is used in long-term orbit propagation problem and showed significant improvement over the *RKN* 12(10) in terms of computational speed.[16] Parallelization of MCPI is then explored and showed a substantial improvement in computational cost over *Matlab ode45* for several initial value problems including a near circular orbit for the classical two-body problem.[17]

Besides all of the above-mentioned widely-used numerical integrators, Eq. (2) can be numerically solved by a wide spectrum of computational methods.[18] These methods in the time domain, such as collocation, finite volume, Galerkin, MLPG, are all essentially branches from the same tree, using the concept of weighted-residual weak-forms, and with different trial and test functions.[19] Among these methods, collocation is one of the simplest and the most efficient ones. A collocation method with harmonic trial functions is developed for studying the periodic responses of nonlinear Duffing oscillators and aeroelastic systems.[20] A time-domain collocation method with Radial Basis Functions as trial function is also developed for direct solution of various time-domain inverse problems such as optimal control and orbital transfer (Lambert's) problems.[21] The method is then extended as a numerical integrator, *RBF-Coll*, for general highly nonlinear systems.[22] The method

is tested against several state of the art explicit and implicit numerical integrators and is shown to be superior in both accuracy and computational cost.[23]

In this study, the previous work of Elgohary et al. is extended to numerically integrate the IVP of the two-body problem, Eq. (1), using Radial Basis Functions and time collocation, *RBF-Coll*, algorithm.[22] An optimization technique is also incorporated to find the best shape parameter for the Radial Basis Functions based on the Leave One Out Cross Validation (LCOOV) algorithm. The method is then compared against *Matlab ode45* and *rkn12(10)* in terms of accuracy, step size and computational cost, for two types of unperturbed orbits; (1) a Low Earth Orbit (LEO) and (2) a High Eccentricity Orbit (HEO). Each set of initial conditions is integrated for 5, 10 and 20 full orbits and the conservation of total energy is used to measure the solution accuracy. The *RBF-Coll* algorithm is also applied to Lambert's problem and a numerical example of the orbit transfer problem is introduced. The analytic *F&G* solution is used as the reference solution and results from all solutions are compared. The examples show the advantages of the present *RBF-Coll* algorithm which enables a much larger time step, and produces high solution accuracy while maintaining a relatively low computational cost.

RADIAL BASIS FUNCTIONS COLLOCATION TIME INTEGRATION

Radial Basis Functions, RBFs, are real-valued functions with values depending on the distance from a source point, $\phi(\mathbf{x}, \mathbf{x}_c) = \phi(\|\mathbf{x} - \mathbf{x}_c\|) = \phi(r)$. Some of the commonly used types for RBFs are:[24]

$$\begin{array}{cc} \phi(r) = e^{-(cr)^2} & \text{Guassian} \\ \phi(r) = \frac{1}{1+(cr)^2} & \text{Inverse quadratic} \\ \phi(r) = \sqrt{1+(cr)^2} & \text{Multiquadric} \\ \phi(r) = \frac{1}{\sqrt{1+(cr)^2}} & \text{Inverse multiquadric} \end{array} \tag{3}$$

where $c > 0$ is the shape parameter.

In this study, the trial functions are expressed as a linear combination of Gaussian functions, with N Legendre-Gauss-Lobatto (LGL) nodes $(t_j, j = 1, \ldots, N)$ as the source points. The LGL nodes can be obtained from solving the differential equation,

$$\left(1 - \tau_j^2\right) \dot{p}_N(\tau_j) = 0 \tag{4}$$

Where, $p_N(\tau)$ are the well known Legendre polynomials orthogonal to the weight function $w(\tau) = 1$ on the interval $\tau \in [-1, 1]$ and satisfy the recursion,

$$\begin{aligned} p_0(\tau) &= 1 \\ p_1(\tau) &= x \\ p_{i+1} &= \left(\frac{2i+1}{i+1}\right) \tau p_i(\tau) - \left(\frac{i}{i+1}\right) p_{i-1}(\tau), \qquad i = 1, 2, \ldots \end{aligned} \tag{5}$$

The solution of Eq. (4) produces the node distribution $-1 = \tau_0 < \tau_1 < \ldots < \tau_N = 1$. The solution is generally obtained by numerical algorithms.[25] By the simple mapping in Eq. (6), $\tau = [-1, \ldots, 1]$ is transformed into $t = [t_0, \ldots, t_F]$ to obtain the LGL nodes for an arbitrary time interval:

$$t = \frac{t_F - t_0}{2} \tau + \frac{t_F + t_0}{2} \tag{6}$$

The collocation is then performed at the N LGL nodes, leading to:

$$\boldsymbol{\chi}(t_i) = \sum_{j=0}^{N} \phi(t_i, t_j)\boldsymbol{\alpha}_j, \quad i = 1, \ldots, N \tag{7}$$

where, α_j is the vector of unknown coefficients at the j-th time step. In matrix-vector form Eq. (7) can be rewritten as,

$$\mathbf{X} = \mathbf{\Phi}\mathbf{A} \tag{8}$$

where $\mathbf{\Phi}$ represents the matrix of basis functions, $\mathbf{A}$ is the vector of undetermined coefficients, and $\mathbf{X}$ is the vector of unknown states at each LGL node. The time-differentiation of Eq. (8) can be then expressed as,

$$\dot{\mathbf{X}} = \dot{\mathbf{\Phi}}\mathbf{A} \tag{9}$$

Hence, combining Eq. (8) and Eq. (9), $\dot{\mathbf{X}}$ is related to $\mathbf{X}$ by,

$$\dot{\mathbf{X}} = D\mathbf{X}, \quad D \equiv \dot{\mathbf{\Phi}}\mathbf{\Phi}^{-1} \tag{10}$$

where, D is called the derivative matrix, which is generated from the RBFs and their time-derivatives evaluated at the LGL nodes.

With the derivative matrix being defined, and with $\boldsymbol{\chi}_{i-1} = \hat{\boldsymbol{\chi}}_{i-1}$ being known from the previous time step, we collocate Eq. (2) at $t_i^2, t_i^3, \ldots, t_i^N$, and collocate the initial condition at t_i^1, leading to the following set of discretized equations:

$$\begin{aligned} &\boldsymbol{\chi}_i^1 - \hat{\boldsymbol{\chi}}_{i-1} = 0 \\ &D\boldsymbol{\chi}_j - \mathbf{g}(\boldsymbol{\chi}_j) = 0, \quad j = 2, 3, \ldots, N \end{aligned} \tag{11}$$

The algorithm as presented above is very simple and easy to implement. The set of nonlinear algebraic equations is solved with the classical Newton's method in this study, whereas other Jacobian-inverse-free methods can also be applied.[26–28] With Eq. (11) being solved, the unknown states at each LGL node, as well as the unknown state at the end of this time interval or step ($\mathbf{x}_i$) are obtained. In this way, the states at each time step within the entire time history, i.e. $t_0, t_1, t_2, \ldots, t_F$ can be numerically evaluated by applying the above numerical algorithm in a sequential procedure.

OPTIMAL SELECTION OF THE SHAPE PARAMETER

The free shape parameter c appearing in most radial basis functions, Eq. (3), has a significant effect on the conditioning of the matrix of basis functions, $\mathbf{\Phi}$. The best results are obtained when c is very small, $c \to 0$. However, this leads to an ill-conditioned matrix and consequently inaccurate results. To overcome such problem Fornberg et al. introduced two methods to stably compute solutions as $c \to 0$; (1) the Contour-Padé method and (2) the RBF-QR method.[29–31] Those methods are shown to successfully overcome the ill-conditioning of the basis functions matrix and to accurately compute the solution at very small values of c. It is still shown that an optimal value of c exists that would result in the most accurate solution.

An algorithm for finding the optimal value of the shape parameter was introduced based on the leave-one-out cross validation (LOOCV) algorithm.[32] The method minimizes a cost function defined by the norm of the error vector evaluated from the difference between the data point and the

interpolant to a reduced data set obtained by removing the point and the corresponding data value. Hence, for a system given by,

$$A\mathbf{x} = \mathbf{b} \tag{12}$$

The error vector to be minimized is given by,

$$e_i = \frac{x_i}{A_{ii}^{-1}} \tag{13}$$

The method is extended to encompass radial basis functions used in pseudo-spectral methods applied to partial differential equations.[33] An algorithm based on the LOOCV is developed and implemented to obtain the optimal shape parameter for the best conditioning of the derivative matrix D with direct implementation in *Matlab*.[33,34] The derivative matrix expression in Eq. (10), can be rewritten as,

$$\mathbf{\Phi} D^{\mathrm{T}} = \dot{\mathbf{\Phi}}^{\mathrm{T}} \tag{14}$$

Which has the same form of the general linear system in Eq. (12) leading to the evaluation of the error matrix as,

$$E_{ij} = \frac{D_{ij}^{\mathrm{T}}}{\mathbf{\Phi}_{ii}^{-1}} \tag{15}$$

In this study, following the work of Fasshauer, the LOOCV algorithm is used to find the optimal value of the shape parameter to evaluate the derivative matrix D. The algorithm is very simple and can be implemented as follows,[32,33]

Algorithm 1 Algorithm for finding optimal shape parameter c

Initial guess of c
Evaluate $\mathbf{\Phi}$
Evaluate $\dot{\mathbf{\Phi}}$
$D = \dot{\mathbf{\Phi}}\mathbf{\Phi}^{-1}$
Error Matrix $= D^{\mathrm{T}}/\mathrm{Diag}[\mathbf{\Phi}^{-1}]$
Find c to Min $\|$Error Matrix$\|$

The minimization presented in the algorithm can be then simply performed via *Matlab* built-in function *fminbnd*.[33,34] It is noted that for the best results one could combine the Contour-Padé method or the RBF-QR method with the shape parameter optimization algorithm. This approach will be pursued in future studies.

ORBIT PROPAGATION PROBLEMS

In this section two examples are presented for the classical/unperturbed two-body problem; (1) a Low Earth Orbit (LEO) with an eccentricity of $e = 0.1$ and (2) a High Eccentricity Orbit (HEO) with $e = 0.7$. Each set of initial conditions is propagated for 20 full orbits and the results are compared against the analytic Lagrange/Gibbs *F&G* solution. The results are also compared against *Matlab* adaptive Runge-Kutta-Fehlberg numerical integrator, *ode45* and the higher order Runge-Kutta-Nyström *RKN*, *rkn12(10)*.[12] For measuring the accuracy the conservation of energy of the orbit is used and the errors are calculated from,

$$\epsilon_k = \left| \frac{E_k - E_0}{E_0} \right| \tag{16}$$

Where, E_0 is the total energy evaluated at the initial conditions and E_k is the total energy at each time step,

$$E_k = \frac{\dot{\mathbf{r}}_k \cdot \dot{\mathbf{r}}_k}{2} - \frac{\mu}{r_k} \tag{17}$$

For better numerical stability, canonical units are used for the presented results. To normalize the gravitational parameter, μ, such that,

$$\hat{\mu} = 1 = \mu \frac{TU^2}{DU^3} \tag{18}$$

The following length and time scales are used for Earth orbits,

$$\begin{aligned} 1DU &= R_e \\ 1TU &= \sqrt{\frac{Re^3}{\mu}} \end{aligned} \tag{19}$$

Where, R_e is the Earth equatorial radius, $R_e = 6378.1$ km and μ the Earth gravitational parameter, $\mu = 398600.4418\ \text{km}^3\text{s}^{-2}$.

Low Earth Orbit

The initial conditions for the Low Earth Orbit (LEO) are

$$\begin{aligned} \mathbf{r} &= \begin{bmatrix} 1.702547136867679 & 6.353992417071098 & 0 \end{bmatrix}^{\mathrm{T}} \times 10^6\,\text{m} \\ \dot{\mathbf{r}} &= \begin{bmatrix} -7.886014053829254 & 2.113051097224035 & 0 \end{bmatrix}^{\mathrm{T}} \times 10^3\,\text{m/s} \end{aligned} \tag{20}$$

The orbit elements are then calculated as,

$$\begin{aligned} a &= 7.30904 \times 10^6\,\text{m} \\ e &= 0.1 \\ i = \Omega = \omega &= 0^\circ \\ T_p &= 6.21872 \times 10^3\,\text{sec} \end{aligned} \tag{21}$$

where a is the semi-major axis, e is the eccentricity, i is the inclination angle, Ω is the longitude of the ascending node, ω is the argument of periapsis, and T_p is the orbit period. Equation (1) is numerically integrated with the present *RBF-Coll* algorithm, *ode45* and *rkn12(10)* for 20 orbits. The total energy errors are shown in Figure 1 for *RBF-Coll*, *ode45*, *rkn12(10)* and the *F&G* analytic solution. Table 1 shows a comparison between *RBF-Coll*, *ode45* and *rkn12(10)* with the *F&G* solution as the reference in terms of accuracy, calculated from the norm of the total energy error vector in Eq. (16) and the simulation time in seconds.

It is shown from Table 1 that the *RBF-Coll* algorithm is more accurate with a lower computational cost when compared to the more optimized *ode45*. The higher order *rkn12(10)* is shown to be superior in the solution accuracy but with a significant increase in the computational cost due to its 17 function calls per time step. In general, the *RBF-Coll* algorithm is shown to be $\approx 3X$ faster than both integrators while maintaining a high solution accuracy.

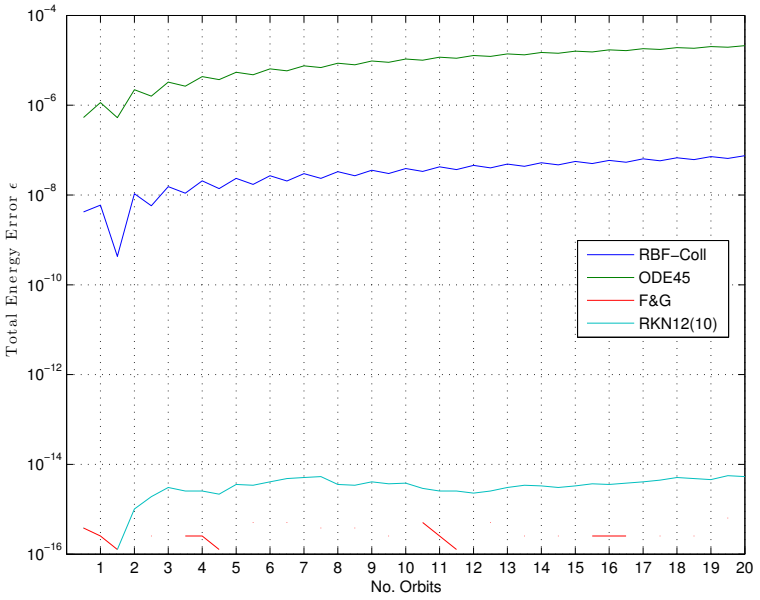

Figure 1. Total Energy Error, LEO

Table 1. Numerical Results Comparison, LEO

Method	Δt	$N/\Delta t$	$\|\epsilon\|$	Sim. Time (sec)
F&G, Orbits $= 5$	$0.5T_p$	N/A	6.61×10^{-16}	N/A
ode45, Orbits $= 5$	Varies	N/A	9.36×10^{-6}	0.21
rkn12(10), Orbits $= 5$	Varies	N/A	6.67×10^{-15}	0.15
RBF-Coll, Orbits $= 5$	$0.5T_p$	18	4.16×10^{-8}	0.051
F&G, Orbits $= 10$	$0.5T_p$	N/A	1.15×10^{-15}	N/A
ode45, Orbits $= 10$	Varies	N/A	2.67×10^{-5}	0.22
rkn12(10), Orbits $= 10$	Varies	N/A	1.48×10^{-14}	0.25
RBF-Coll, Orbits $= 10$	$0.5T_p$	18	1.01×10^{-7}	0.075
F&G, Orbits $= 20$	$0.5T_p$	N/A	1.66×10^{-15}	N/A
ode45, Orbits $= 20$	Varies	N/A	7.65×10^{-5}	0.27
rkn12(10), Orbits $= 20$	Varies	N/A	2.3×10^{-14}	0.31
RBF-Coll, Orbits $= 20$	$0.5T_p$	18	2.65×10^{-7}	0.13

High Eccentricity Orbit

The initial conditions for the High Eccentricity Orbit (HEO) are given by

$$\begin{aligned} \mathbf{r} &= \begin{bmatrix} 2.096434265330419 & 7.823999192941453 & 0 \end{bmatrix}^{\mathrm{T}} \times 10^6 \,\mathrm{m} \\ \dot{\mathbf{r}} &= \begin{bmatrix} -8.834757074967362 & 2.367266023562654 & 0 \end{bmatrix}^{\mathrm{T}} \times 10^3 \,\mathrm{m/s} \end{aligned} \tag{22}$$

With the classical orbit elements,

$$\begin{aligned} a &= 2.7 \times 10^7 \,\mathrm{m} \\ e &= 0.7 \\ i &= 0^\circ \\ \Omega &= 45^\circ \\ \omega &= 30^\circ \\ T_p &= 4.41526 \times 10^4 \,\mathrm{sec} \end{aligned} \tag{23}$$

As in the previous section, Eq. (1) is numerically integrated with the present *RBF-Coll* algorithm, *ode45* and *rkn12(10)* for 20 orbits. The total energy errors are shown in Figure 2 for the numerical integrators and the analytic *F&G* solution. Table 2 shows the comparison between *RBF-Coll*, *ode45* and the *F&G* solution. The comparison is again shown for 5, 10 and 20 orbits.

As shown in Table 2, the optimized adaptive nature of *ode45* proved useful when it comes to the computational cost comparison for 20 orbits. The *RBF-Coll* algorithm however, is still more accurate across all experiments and with acceptable computational cost when compared to *ode45*. The *rkn12(10)* is the most accurate but with almost two times the computational cost of the *RBF-Coll* across all experiments. Essentially, the RBF-Coll algorithm is a fixed step size, implicit numerical integrator. The step size had to be decreased and the number of nodes had to be increased to account for the very high eccentricity of the orbit while maintaining solution accuracy. By developing an adaptive *RBF-Coll* algorithm the trade-off between the accuracy, the number of nodes and the step size can be explored to further improve the overall computational cost of the algorithm.

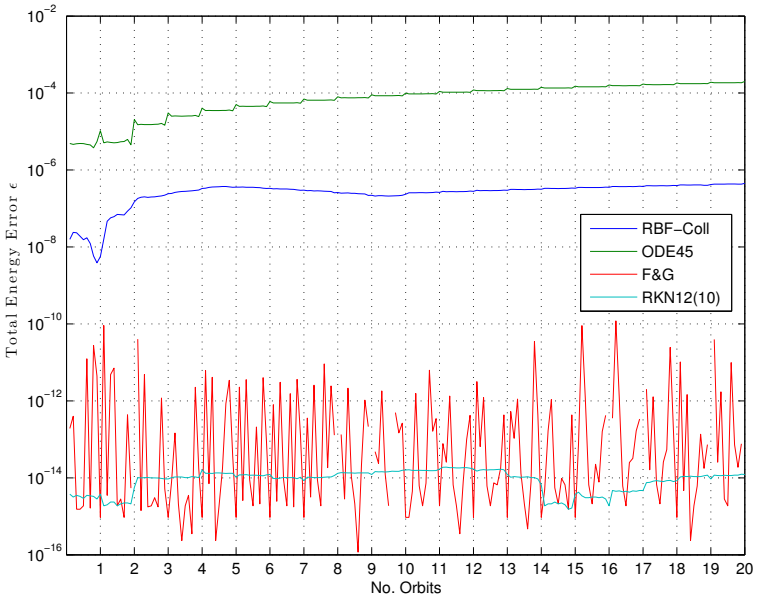

Figure 2. Total Energy Error, HEO

Table 2. Numerical Results Comparison, HEO

Method	Δt	$N/\Delta t$	$\|\epsilon\|$	Sim. Time (sec)
F&G, Orbits $= 5$	$0.1T_p$	N/A	1.05×10^{-10}	N/A
ode45, Orbits $= 5$	Varies	N/A	1.58×10^{-4}	0.202
rkn12(10), Orbits $= 5$	Varies	N/A	6.5×10^{-14}	0.29
RBF-Coll, Orbits $= 5$	$0.1T_p$	27	1.59×10^{-6}	0.15
F&G, Orbits $= 10$	$0.1T_p$	N/A	1.054×10^{-10}	N/A
ode45, Orbits $= 10$	Varies	N/A	5.08×10^{-4}	0.26
rkn12(10), Orbits $= 10$	Varies	N/A	1.5×10^{-13}	0.51
RBF-Coll, Orbits $= 10$	$0.1T_p$	27	2.52×10^{-6}	0.26
F&G, Orbits $= 20$	$0.1T_p$	N/A	1.925×10^{-10}	N/A
ode45, Orbits $= 20$	Varies	N/A	1.533×10^{-3}	0.34
rkn12(10), Orbits $= 20$	Varies	N/A	1.5×10^{-13}	0.77
RBF-Coll, Orbits $= 20$	$0.1T_p$	27	4.32×10^{-6}	0.5

ORBIT TRANSFER PROBLEMS

The fixed-time two-point boundary value problem of orbit transfer is a classical problem in celestial mechanics. This problem is known as Lambert's problem after Johann Heinrich Lambert (1728–1779) who was the first to state and to solve the problem. The objective is to find the transfer orbit that connects two points in space given a flight time. Figure 3 illustrates the geometry of Lambert's problem with $t_0, \mathbf{r}_0$ the initial time and position, $t_F, \mathbf{r}_F$ the desired final time and position, $\mathbf{v}_0$ the initial velocity to be solved for that would generate the transfer orbit and $\mathbf{v}_F$ the terminal velocity at the desired position.

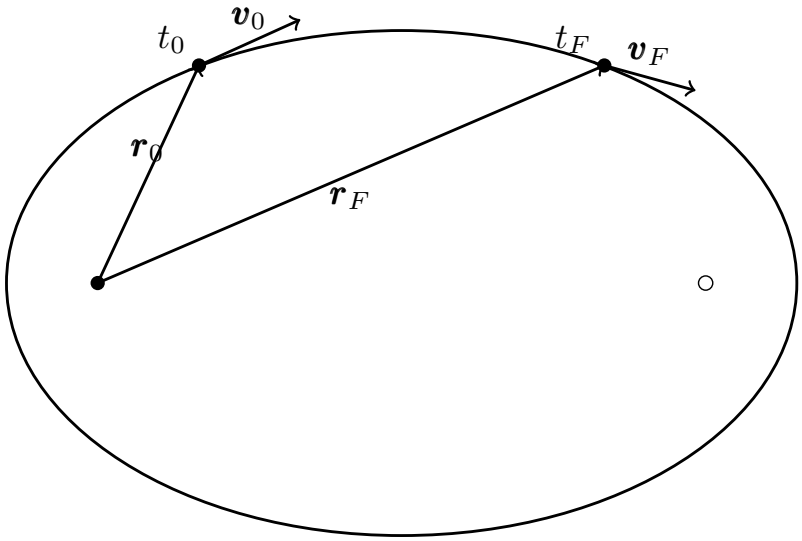

Figure 3. Illustration of Lambert's Problem

The dynamics of the unperturbed relative two-body problem in Eq. (1) applies and the analytical solution for the unperturbed Lambert's problem was discussed in detail.[1] The solution developed

still has a singularity for transfer angles of $\pm 180^{\circ}$. A numerical iterative method is introduced to handle both singularities and gravitational perturbations in Lambert's problem.[2] The method is essentially a shooting algorithm where a sufficiently good initial guess for the initial velocity is needed to improve convergence. Generally, the initial guess for the velocity vector is obtained such that the target position is reached but not necessarily in the required transfer time. The present solution based on *RBF-Coll* starts with an arbitrary initial guess, and can readily handle any perturbations to provide a solution for the transfer orbit problem.

The *RBF-Coll* algorithm can be then applied to the first order system of Eq. (2) to produce a set of $6N$ nonlinear algebraic equations where N is the number of LGL collocation nodes:

$$\begin{aligned}
R_1^i &= Dx_1^i - x_2^i = 0 \\
R_2^i &= Dy_1^i - y_2^i = 0 \\
R_3^i &= Dz_1^i - z_2^i = 0 \\
R_4^1 &= x_1^1 - x_{10} = 0 \\
R_4^j &= Dx_2^j + \frac{\mu}{r^j} x_1^j = 0 \\
R_4^N &= x_1^N - x_{1F} = 0 \\
R_5^1 &= y_1^1 - y_{10} = 0 \\
R_5^j &= Dy_2^j + \frac{\mu}{r^j} y_1^j = 0 \\
R_5^N &= y_1^N - y_{1F} = 0 \\
R_6^1 &= z_1^1 - z_{10} = 0 \\
R_6^j &= Dz_2^j + \frac{\mu}{r^j} z_1^j = 0 \\
R_6^N &= z_1^N - z_{1F} = 0
\end{aligned} \tag{24}$$

where, $i = 1, \ldots, N$ and $j = 2, \ldots, N-1$ which produces a system of $6N$ equations in $6N$ unknowns. As a numerical example an orbit is examined with initial and final position given by,

$$\begin{aligned}
\mathbf{r}_0 &= \begin{bmatrix} 2.87 & 5.19 & 2.85 \end{bmatrix}^{\mathrm{T}} \times 10^6 \,\mathrm{m} \\
\mathbf{r}_F &= \begin{bmatrix} 2.09 & 7.82 & 0 \end{bmatrix}^{\mathrm{T}} \times 10^6 \,\mathrm{m}
\end{aligned} \tag{25}$$

The transfer time is chosen to be $t_F = 0.05$ days or $t_F = 4.32 \times 10^3$ seconds. The number of LGL nodes is set as, $N = 36$ and the whole transfer orbit is solved in one time step equals to the prescribed transfer time. The set of nonlinear algebraic equations in Eq. (24) is solved with an arbitrary initial guess and the resulting orbit is compared against the closed form *F&G* solution considering the initial position and velocity vector obtained from the *RBF-Coll* algorithm. The resulting position and velocity are compared in Figure 4 and Figure 5, respectively.

The errors of the initial and the terminal boundary conditions are compared in Table 3. The initial conditions obtained by the *RBF-Coll* method drives the object to the desired final position with very high accuracy. This approach using *RBF-Coll* thus is quite advantageous compared to previous analytical and numerical methods of solving the Lambert's problem. And it can be extended in future to to address perturbations and obtain what is known as pork-chop plots for the selection of launch and arrival times while minimizing fuel or some other specified parameters.

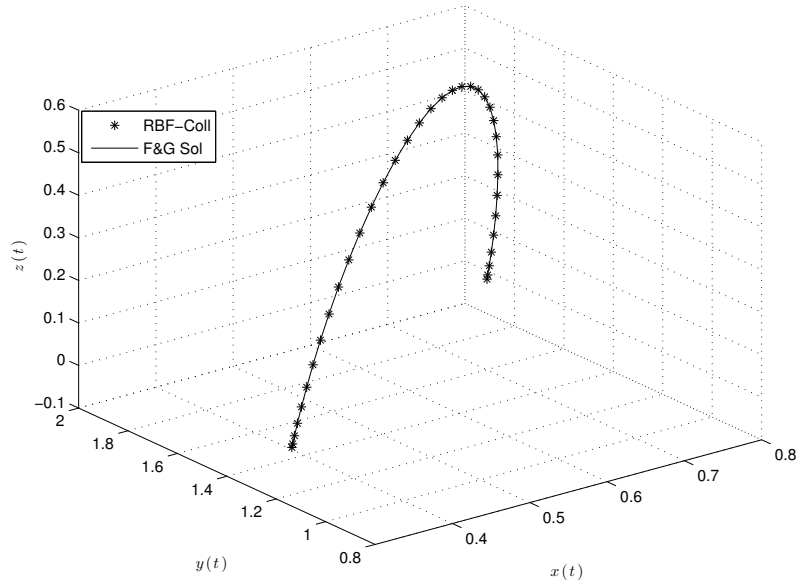

Figure 4. Transfer Orbit Position

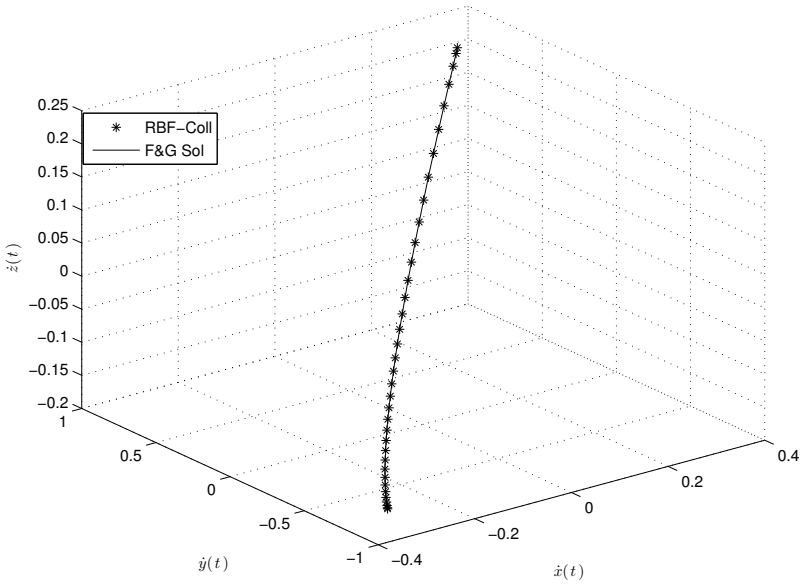

Figure 5. Transfer Orbit Velocity

Table 3. Errors in Boundary Conditions

Initial Boundary Error	Terminal Boundary Error
$\begin{Bmatrix} 0 \\ 0 \\ 0 \end{Bmatrix}$	$\begin{Bmatrix} 1.510^{-7} \\ 4.3 \times 10^{-7} \\ 7.7 \times 10^{-8} \end{Bmatrix}$

DISCUSSION & CONCLUSION

The present *RBF-Coll* algorithm is shown to be highly accurate, fast and very simple to implement for long-term orbit propagation and orbit transfers of the classical two-body problem. The comparison against *Matlab ode45* and *rkn12(10)* shows the advantages of the *RBF-Coll* algorithm that enables larger step-size with relatively high solution accuracy while maintaining low computational cost. The case of twenty complete HEO orbits shows the potential of the algorithm for adaptive step size schemes. Moreover, combining the basis matrix decomposition algorithms with the optimal shape parameter can further enhance accuracy and lower computational cost by lowering the number of nodes required per time step. The algorithm also handled the orbit transfer problem with very high accuracy and arbitrary initial guess. Gravitational perturbations can also be easily handled with the *RBF-Coll* algorithm. Areas of studies that will be explored in future works.

REFERENCES

[1] R. Battin, *An introduction to the mathematics and methods of astrodynamics*. AIAA, 1987.

[2] H. Schaub and J. Junkins, *Analytical mechanics of space systems*. AIAA, 2003.

[3] J. D. Turner, T. A. Elgohary, M. Majji, and J. L. Junkins, "High accuracy trajectory and uncertainty propagation algorithm for long-term asteroid motion prediction," *Adventures on the Interface of Mechanics and Control* (K. Alfriend, M. Akella, J. Hurtado, and J. Turner, eds.), pp. 15–34, Tech Science Press, 2012.

[4] T. A. Elgohary, J. D. Turner, and J. L. Junkins, "High-Order Analytic Continuation and Numerical Stability Analysis for the Classical Two-Body Problem," *Advances in Astronautical Sciences: The Jer-Nan Juang Astrodynamics Symposium*, Vol. 147, 2012, pp. 627–646.

[5] T. A. Elgohary and J. D. Turner, "State Transition Tensor Models for the Uncertainty Propagation of the Two-Body Problem," *Advances in Astronautical Sciences: AAS/AIAA Astrodynamics Conference*, Vol. 150, 2014, pp. 1171–1194.

[6] J. D. Turner and T. A. Elgohary, "Analytic Orbit Trajectory Prediction for J2-J6 Using Recursive Lagrange-Like Invariants," *Advanced Maui Optical and Space Surveillance Technologies Conference*, Vol. 1, 2013, p. 108.

[7] K. Hernandez, J. L. Read, T. A. Elgohary, J. D. Turner, and J. L. Junkins, "Analytic Power Series Solutions for Two-body and J2–J6 Trajectories ans State Transition Models," *Advances in Astronautical Sciences: AAS/AIAA Astrodynamics Specialist Conference*, 2015.

[8] E. Fehlberg, "Low-order classical Runge-Kutta formulas with stepsize control and their application to some heat transfer problems," tech. rep., NASA, 1969.

[9] S. Filippi and J. Gräf, "New Runge–Kutta–Nyström formula-pairs of order 8 (7), 9 (8), 10 (9) and 11 (10) for differential equations of the form $y" = f(x, y)$," *Journal of computational and applied mathematics*, Vol. 14, No. 3, 1986, pp. 361–370.

[10] K. Fox, "Numerical integration of the equations of motion of celestial mechanics," *Celestial mechanics*, Vol. 33, No. 2, 1984, pp. 127–142.

[11] M. M. Berry and L. M. Healy, "Implementation of Gauss-Jackson integration for orbit propagation," *The Journal of the Astronautical Sciences*, Vol. 52, No. 3, 2004, pp. 331–357.

[12] J. Dormand, M. El-Mikkawy, and P. Prince, "High-order embedded Runge-Kutta-Nystrom formulae," *IMA Journal of Numerical Analysis*, Vol. 7, No. 4, 1987, pp. 423–430.

[13] O. Montenbruck, "Numerical integration methods for orbital motion," *Celestial Mechanics and Dynamical Astronomy*, Vol. 53, No. 1, 1992, pp. 59–69.

[14] K. Hadjifotinou and M. Gousidou-Koutita, "Comparison of numerical methods for the integration of natural satellite systems," *Celestial Mechanics and Dynamical Astronomy*, Vol. 70, No. 2, 1998, pp. 99–113.

[15] P. W. Sharp, "N-body simulations: The performance of some integrators," *ACM Transactions on Mathematical Software (TOMS)*, Vol. 32, No. 3, 2006, pp. 375–395.

[16] X. Bai and J. L. Junkins, "Modified Chebyshev-Picard Iteration Methods for Orbit Propagation," *The Journal of the Astronautical Sciences*, Vol. 58, No. 4, 2011, pp. 583–613.

[17] X. Bai and J. L. Junkins, "Modified Chebyshev-Picard iteration methods for solution of initial value problems," *The Journal of the Astronautical Sciences*, Vol. 59, No. 1-2, 2012, pp. 335–359.

[18] S. N. Atluri, *Methods of computer modeling in engineering & the sciences*, Vol. 1. Tech Science Press Palmdale, 2005.

[19] L. Dong, A. Alotaibi, S. Mohiuddine, and S. Atluri, "Computational methods in engineering: a variety of primal & mixed methods, with global & local interpolations, for well-posed or ill-Posed BCs," *CMES: Computer Modeling in Engineering & Sciences*, Vol. 99, No. 1, 2014, pp. 1–85.

[20] H.-H. Dai, M. Schnoor, and S. N. Atluri, "A simple collocation scheme for obtaining the periodic solutions of the Duffing equation, and its equivalence to the high dimensional harmonic balance method: subharmonic oscillations," *Computer Modeling in Engineering and Sciences*, Vol. 84, No. 5, 2012, pp. 459–497.

[21] T. A. Elgohary, L. Dong, J. L. Junkins, and S. N. Atluri, "Time Domain Inverse Problems in Nonlinear Systems Using Collocation & Radial Basis Functions," *CMES: Computer Modeling in Engineering & Sciences*, Vol. 100, No. 1, 2014, pp. 59–84.

[22] T. A. Elgohary, L. Dong, J. L. Junkins, and S. N. Atluri, "A Simple, Fast, and Accurate Time-Integrator for Strongly Nonlinear Dynamical Systems," *CMES: Computer Modeling in Engineering & Sciences*, Vol. 100, No. 3, 2014, pp. 249–275.

[23] T. A. Elgohary, *Novel Computational and Analytic Techniques for Nonlinear Systems Applied to Structural and Celestial Mechanics*. PhD thesis, Texas A&M University, 2015.

[24] M. D. Buhmann, *Radial basis functions: theory and implementations*, Vol. 5. Cambridge university press Cambridge, 2003.

[25] G. N. Elnagar and M. A. Kazemi, "Pseudospectral Legendre-based optimal computation of nonlinear constrained variational problems," *Journal of computational and applied mathematics*, Vol. 88, No. 2, 1998, pp. 363–375.

[26] C. S. Liu, W. Yeih, C. L. Kuo, and S. N. Atluri, "A scalar homotopy method for solving an over/under determined system of non-linear algebraic equations," *Computer Modeling in Engineering and Sciences*, Vol. 53, No. 1, 2009, pp. 47–71.

[27] C.-S. Liu and S. N. Atluri, "A Globally Optimal Iterative Algorithm Using the Best Descent Vector $\dot{\mathbf{x}} = \lambda\left[\alpha_c\mathbf{F} + \mathbf{B}^{\mathbf{T}}\mathbf{F}\right]$, with the Critical Value α_c, for Solving a System of Nonlinear Algebraic Equations $\mathbf{F}(\mathbf{x}) = \mathbf{0}$," *Computer Modeling in Engineering and Sciences*, Vol. 84, No. 6, 2012, p. 575.

[28] T. A. Elgohary, L. Dong, J. L. Junkins, and S. N. Atluri, "Solution of Post-Buckling & Limit Load Problems, Without Inverting the Tangent Stiffness Matrix & Without Using Arc-Length Methods," *CMES: Computer Modeling in Engineering & Sciences*, Vol. 98, No. 6, 2014, pp. 543–563.

[29] B. Fornberg and G. Wright, "Stable computation of multiquadric interpolants for all values of the shape parameter," *Computers & Mathematics with Applications*, Vol. 48, No. 5, 2004, pp. 853–867.

[30] B. Fornberg and C. Piret, "A stable algorithm for flat radial basis functions on a sphere," *SIAM Journal on Scientific Computing*, Vol. 30, No. 1, 2007, pp. 60–80.

[31] B. Fornberg, E. Larsson, and N. Flyer, "Stable computations with Gaussian radial basis functions," *SIAM Journal on Scientific Computing*, Vol. 33, No. 2, 2011, pp. 869–892.

[32] S. Rippa, "An algorithm for selecting a good value for the parameter c in radial basis function interpolation," *Advances in Computational Mathematics*, Vol. 11, No. 2-3, 1999, pp. 193–210.

[33] G. E. Fasshauer and J. G. Zhang, "On choosing optimal shape parameters for RBF approximation," *Numerical Algorithms*, Vol. 45, No. 1-4, 2007, pp. 345–368.

[34] G. F. Fasshauer, *Meshfree approximation methods with MATLAB*. World Scientific Publishing Co., Inc., 2007.